A 3D MODEL FOR SNOW DRIFT AND SNOW COVER DEVELOPMENT IN STEEP ALPINE TERRAIN

Michael Lehning*, Judith Doorschot, Charles Fierz and Norbert Raderschall
WSL, Swiss Federal Institute for Snow and Avalanche Research, SLF

ABSTRACT: Since blowing and drifting snow is a major factor influencing avalanche danger and the local micro climate, a high resolution, objective and quantitative assessment and forecast of snow transport by wind is of great practical value. Wind transport of snow is governed by three components: the erodability of the snow pack, the current snowfall and the wind field. A snowdrift model has been developed that combines an atmospheric model analysis of the high resolution wind field over steep topography, a novel formulation for snow drift and a snow cover model. For modeling snow drift, the transport modes saltation and suspension are distinguished.

This presentation focuses on the model parts describing snow drift and snow cover. The snow cover is represented by the numerical model SNOWPACK. A novel model for snow saltation is presented, which is suitable for steep terrain. Based on a computationally efficient equilibrium approach, the description of saltation uses explicit trajectory calculations to estimate mass fluxes on steep slopes. Emphasis of the presentation is further on the coupling between the snow cover, the drifting and blowing snow and the wind field. For a correct description of the erosion and deposition pattern, the formulation of the coupling functions is of major importance.

The model system is applied to predict snow loading in avalanche slopes. Results for the avalanche winter 1998 / 1999 are presented. The evaluation of these results show that major characteristics of snow redistribution are captured by the model. In steep terrain, saltation appears to contribute less to snow redistribution than previously assumed. Preferential deposition during snow fall events appears to be a major factor influencing snow distribution in small scale steep terrain. Remaining uncertainties of the model system concern the formulation of suspension and the accuracy of the flow simulation. Suggestions for improvements are made.

KEYWORDS: ARPS, lee slope, avalanches, wind slab, flow simulation, saltation, suspension, erosion, snow preferential deposition

1. INTRODUCTION

Snow transport by wind is a spectacular phenomenon. It crucially influences the seasonal build-up of the snow cover in Alpine terrain and the related avalanche activity. But it also influences growth of vegetation and storage of water and pollutants. Because of its importance, snow drift has been studied extensively over the last few decades, and a lot of progress has been made in modeling and understanding of snow drift. Despite these efforts, complete descriptions of snow redistribution by the wind hardly exist due to the complexity of the physical processes associated with this phenomenon. The development of complete models is of extreme interest for the improvement of avalanche forecasting.

* *Corresponding author address:* Michael Lehning, Swiss Federal Institute for Snow and Avalanche Research, Flüelastr. 11, CH – 7260 Davos, Switzerland; tel: ++41 81 417 0158; email: lehning@slf.ch

Traditionally, snow drift research has been motivated by engineering applications to mitigate the adverse effects of blowing and drifting snow or to assess the mass and energy balance of snow and ice surfaces in high latitudes (Andreas, 1995; Bintanja et al., 1995; Wamser and Lykossov, 1995; King et al., 1996; Déry et al., 1998; Sundsbø 1998; Mann et al., 2000; Gallée et al., 2001). Recently, modeling efforts have been intensified, trying to describe the effects of drifting snow on the atmospheric boundary layer (Xiao et al., 2000; Bintanja, 2000; Déry et al., 2001). Those models are highly parameterized descriptions of the physical processes involved in snow drift.

Snow drift research in Alpine areas is complicated by the steep terrain. A first study of wind transport of snow over alpine crests was initiated by Föhn (1980) working at the Gaudergrat ridge in the Davos region. He emphasized some peculiarities of the wind field at this elongated crest and quantified snow transport over the crest. Föhn and Meister (1983) published a continuation of this work where they analyzed specific distribution patterns of ablation and deposition for quasi two-dimensional ridges with a predominant wind flow perpendicular to the crest. A further extension and re-evaluation is the work of Meister (1987), which focuses on the wind profile over the crest and the associated snow transport.

In the model of Green et al. (1999), which is based on Liston and Sturm (1998), advective terms are not adequately taken into account, and it can only be used for gentle topographies. More advanced models have been developed by Naaim et al. (1998) and Uematsu (1993), however in neither of these models the preferential deposition of precipitation is included.

With the dissertation of Gauer (2001), a new phase of snow drift research has been initiated at the SLF. Working with a commercially available flow solver (CFX 4.1) and a detailed physical model of blowing snow distinguishing between a saltation and a suspension layer, very high resolution (up to 5 m) simulations of snow drift have been performed for the Gaudergrat site and evaluated against field measurements. For this purpose the Gaudergrat ridge had been equipped with six meteorological masts. While Gauer's results were encouraging, critical features of wind field and snow distribution such as flow separation and a wavy deposition pattern in the lee slope could not be reproduced by this model system.

Therefore, a different and more modular approach is now implemented. Based on the non-hydrostatic meteorological model ARPS, wind and turbulence fields are calculated. Separate model modules are developed for saltation, suspension and snow cover development. This paper presents an overview of the model system and emphasizes the importance of suspension and preferential deposition in steep terrain.

2. MODEL SUMMARY

2.1. Flow Simulation

For obtaining the high resolution wind and turbulence fields over complex topography we use the mesoscale atmospheric model ARPS (Advanced Regional Prediction System). In ARPS, the non-hydrostatic compressible Navier-Stokes equations for a turbulent air flow are solved on a numerical mesh, using the finite differences method. Novel is the use of a mesoscale atmospheric model with a resolution down to 25 m in the presented case. First details on the flow field simulation and background on ARPS are available from Raderschall et al. (2002).

2.2. Saltation

For calculating the snow mass that is transported in the saltation layer, we introduce a new physical model. One of its new features is the consideration of the influence of a sloping bottom. Also new is the consideration of snow grain elasticity during impact. Note that current empirical snow saltation models (e.g. Pomeroy and Gray, 1990) are only valid over flat terrain and do not consider grain or surface properties. Furthermore, the effects of particle-wind feedback, particle trajectories and grain properties are included in the new formulation. The model has been shown to correctly simulate measured saltation fluxes of snow. All model details are given in Doorschot and Lehning (2002).

2.3. Suspension and preferential deposition

Particle transport in suspension from drift and snow fall can be treated identically. The suspended particles are treated as passive tracers of the wind field, and no effects of turbulence damping or interaction between particles are considered.

The conservation of particle mass yields:

$$\frac{\partial c}{\partial t} + u\frac{\partial c}{\partial x} + v\frac{\partial c}{\partial y} + (w - w_s)\frac{\partial c}{\partial z} = 0, \qquad (1)$$

where c (kg m^{-3}) denotes the moisture concentration, and w_s the settling velocity. Phase changes are not considered. For the settling velocity, a parameterization is derived taking into account turbulence effects. In non-moving air the settling velocity w_{s0} is governed by a balance between friction and gravity, resulting in (Stokes law):

$$w_{s0} = \frac{\rho_p d^2 g}{18\eta}. \qquad (2)$$

Here g is the acceleration due to gravity and η the friction coefficient of air (viscosity). We make the assumption that the settling velocity in a turbulent air flow equals its value in still air minus a term to account for the turbulence:

$$w_s = w_{s0} - w_t. \qquad (3)$$

For obtaining the term w_t, we turn to the definition of the turbulent kinetic energy per unit mass, e:

$$e = 0.5(\overline{u'^2} + \overline{v'^2} + \overline{w'^2}), \quad (4)$$

where the dashed variables denote the deviations from average of the respective velocities. Using a scaling approach, we can link w_t to e and receive for symmetric turbulence:

$$w_t = \sqrt{\overline{w'^2}} = \sqrt{2/3\, e}. \quad (5)$$

Thus, the total settling velocity w_s is given by:

$$w_s = \frac{\rho_p d^2 g}{18\eta} - \sqrt{2/3\, e}. \quad (6)$$

Using surface layer similarity (Stull, 1988), Eq. (6) can also be expressed in terms of the friction velocity:

$$w_s = \frac{\rho_p d^2 g}{18\eta} - \sqrt{10/3}\, u_*. \quad (7)$$

The turbulent kinetic energy is obtained directly from the wind field simulations for every grid point, which allows the computation of the turbulent settling velocity.

At the upper boundary of the domain, the boundary condition (BC) for the particle concentration is given by the precipitation rate. At the lower boundary, the concentrations are not prescribed but are left variable. They develop as a result of transport in suspension and saltation. The influence of saltation on the concentrations at the lower boundary is detailed in section 2.5.

2.4. The snow module SNOWPACK

SNOWPACK is the finite-element based physical snow cover model of the Swiss Federal Institute for Snow and Avalanche Research (SLF), which is in operational use in connection with the Swiss network of approximately 90 high Alpine automatic snow and weather stations, Lehning et al. (1999). It solves the instationary heat transfer and snow settlement equations and calculates phase changes and transport of water vapor and liquid water. Furthermore, it includes surface hoar formation and snow metamorphism (grain types). A complete description of the model can be found in Lehning and Bartelt (2002), Lehning et al. (2002a) and Lehning et al. (2002b). For the present purpose, SNOWPACK has been coupled to our snow drift model for the assessment of the erodability of the snow cover (Lehning et al., 2000a) and the development of the snow cover at different locations due to erosion and deposition of snow.

2.5. Model Coupling

The individual model modules deliver wind and turbulence, saltation fluxes, a description of suspension and the snow cover development. These parts need to be coupled.

At present, the flow simulation (ARPS) receives no feed-back from the remaining parts. It can be run separately to produce the flow fields. Since it is known that drifting snow influences exchange of energy and momentum and that surface roughness and height is altered by the snow, we intend to introduce a two way coupling in a later version. Note the use of a wall function with particle – flow feed back in the saltation model (2.2), however. Our high spatial grid resolution also requires a high time resolution of the order of 0.1 s for the flow simulations. This results in long computation times for the simulation of real snow drift events. Therefore, we have adopted the following simplified procedure: For chosen time intervals (at present one hour), we model an representative (stationary) wind field with ARPS using the time-averaged measurements to prescribe initial and boundary conditions. Additional meteorological parameters such as precipitation rates, temperature and humidity are taken from measurements. From ARPS, the turbulent kinetic energy (TKE) and 3-dimensional wind velocity is then known at every grid point and for every hour of the simulation period.

The remaining modules of the model system are fully coupled and run simultaneously. The first step is to initialize the snow cover, to read the flow field for the first hour and to initialize the suspension concentrations. The following procedure is then repeated for each computational time step. First, the suspension equation (1) is solved. The suspension model calculates for the given (stationary) wind conditions the concentration distribution for all grid points until a steady state is reached. Then the saltation fluxes are calculated for all surface grid points, for which the threshold wind speed is exceeded. From this result, a particle concentration at the height of the saltation layer is calculated. For this purpose, we consider the energy balance of the system. At saltation height, h_s, the wind velocity shows a deviation from the logarithmic profile, $\Delta U(h_s)$, due to the energy that has been transferred to the saltating particles. Thus the particle concentration c_p can be expressed as a function of this wind velocity deficit, the air density, ρ_a, and the mean speed of the particles in saltation, u_{mean}:

$$c_p(z = h_s) = \frac{\rho_a(\Delta U(h_s))^2}{u_{mean}^2}. \quad (8)$$

This concentration is one part for a mass balance for the saltation layer. At steady state, the divergence of the horizontal saltation flux, Q^*, must be balanced by grains entering and leaving the saltation layer from the snow surface, $F_z(0)$, and from the suspension layer above, $F_z(h_s)$. Formulated for a finite volume (Δx, Δy, $\Delta z=h_s$), this yields:

$$0 = \frac{\Delta Q^*}{\Delta x} + \frac{\Delta Q^*}{\Delta y} + F_z(h_s) + F_z(0). \quad (9)$$

The horizontally projected saltation flux is obtained by considering the slope angle in direction of the mean wind vector, α:

$$Q^* = Q\cos(\alpha). \quad (10)$$

The mass exchange between the saltation and suspension layer is parameterized in the following form:

$$F_z(h_s) = c\ (w_s - fw). \quad (11)$$

In (11), c is the concentration of snow at the lowest node *above* the surface in the element mesh for the solution of Eq. (1). Also the vertical settling velocity, w_s and the vertical flow velocity, w, are taken from this layer above the surface. The empirical factor f takes into account that vertical velocities of the flow are much larger at this (higher) level above the surface than at the true height of the saltation layer, h_s. For the simulations presented here, f is set to 0.5.

The influence of the underlying saltation layer (when present) on the concentration c, i.e. the saltation layer as lower boundary condition for the suspension layer is established in the following way: Before solving (1), the concentration at the height of the saltation layer at the current time step as given by Eq. (8), $c_p(t,h_s)$, is added to the concentrations at the lower boundary, c. At the same time, the saltation concentration from the previous time step), $c_p(t-\Delta t,h_s)$, is subtracted:

$$c^{initial}(t) = c(t) + c_p(t,h_s) - c_p(t-\Delta t,h_s). \quad (12)$$

The concentrations obtained after the solution of Eq. (1), $c^{end}(t)$, are then again used in Eq. (11) for the next time step.

By solving Eq. (9), the erosion and deposition of snow at the surface, $F_z(0)$, is determined and used as the mass change input for the SNOWPACK calculations. The wind values are taken directly from ARPS and at present it is assumed that air temperature and relative humidity are constant throughout the domain. The one-dimensional SNOWPACK model is calculated at every surface grid point.

3. RESULTS AND DISCUSSION

Below we present an analysis of snow drift over the Gaudergrat ridge from the first major drift event of the avalanche period 1999 and compare the model results to manual measurements. The simulated period starts on January 26 and ends on January 31. For this period, the snow height development has also been measured.

3.1. Flow Simulation

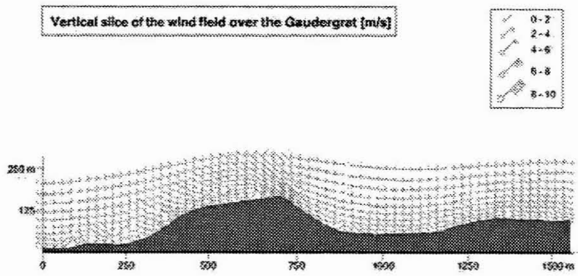

Figure 1: Cross section showing wind vectors on the lowest ten grid levels over the Gaudergrat ridge. The speed-up at the ridge is clearly visible.

The computational grid covers an area of 1.5 x 1.5 km. A cross sectional representation of the topography and the vertical grid levels is found in Figure 1. The wind simulation is for January 29. The lowest grid cell has a vertical extent between 1 m at ridges and summits and 10 m at the flat boundaries. The horizontal resolution is 25 m and 30 vertical layers are calculated to a height of 5000 m a.s.l. The internal calculation time step for ARPS is 0.1 s and we calculate a stationary wind field for each hour between 26.01.1999 12:00 and 31.01.1999 12:00. The time step for calculating saltation and snow cover status is 1 hour. A time step of 1 s for calculating suspension is found to be sufficient to ensure numerical stability. Typically after 10 to 20 iterations the concentration field will become stationary for a given wind field.

3.1. Overall Snow Transport

In Figure 2, a cross section comparison between measured and modeled snow depth changes is shown. The general pattern of luff erosion and lee deposition is correctly simulated, i.e. the model recognizes the erosion in the luff and a series of deposition maxima in the lee due to lee rotors. Even the approximate location of the maxima can be calculated with the resolution of 25 m. However, it is also evident that a resolution of 25 m is not yet sufficient to simulate the small scale snow erosion and deposition pattern. The overall amount of transported snow is well reproduced. More results on the erosion and deposition patterns are found in Lehning et al. (2000b).

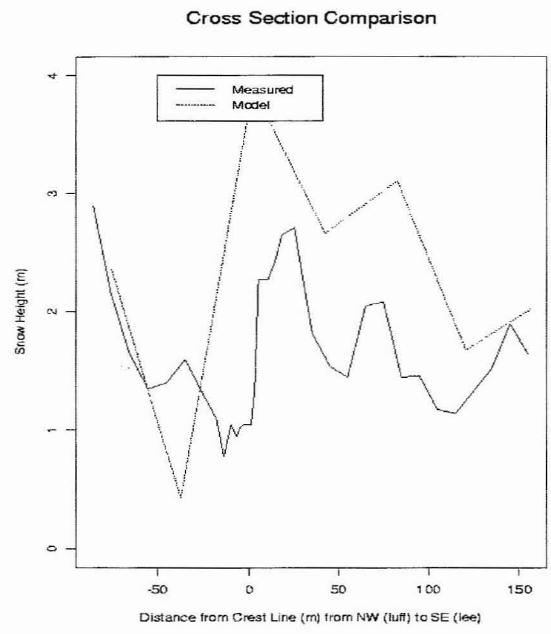

Figure 2: Comparison between measured and simulated snow depth changes following a transect over the Gaudergrat ridge for the storm period 26. – 31. January 1999. The simulation reproduces important features of snow deposition and erosion but is limited by the spatial resolution of 25 m.

3.3. Saltation, Suspension and Preferential Deposition

The remarkable agreement between measured and simulated snow distribution motivates us to investigate the individual processes of snow transport in more detail. In particular, since preferential deposition is not included in most current snow drift models, we emphasize the role of this mechanism in creating variable snow deposition in complex terrain.

Preferential deposition is the process of an uneven deposition of snow precipitation over complex terrain. Because of the turbulent flow over hills and mountains with speed-up, separation and up- and downdraft zones, snow is non-uniformly deposited even at wind velocities too small to exceed the threshold for the onset of saltation. Thus, over hills and mountains, snow drift features will occur even in the absence of erosion of deposited snow.

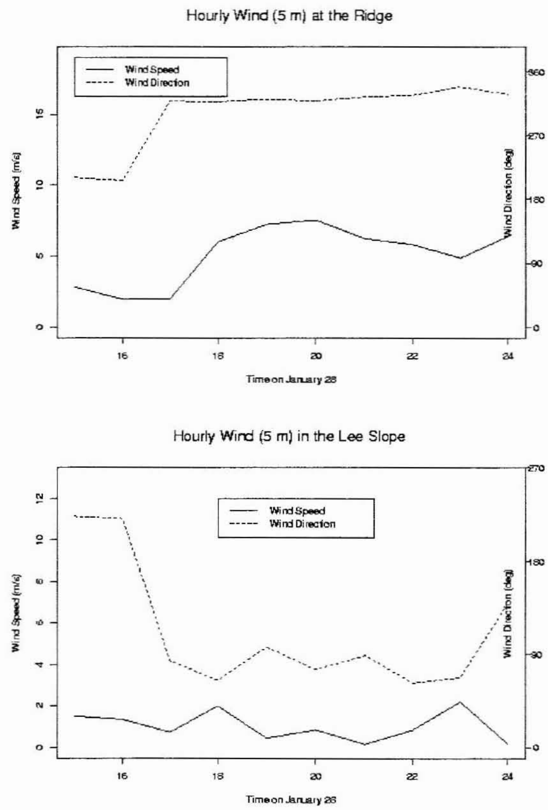

Figure 3: Measured wind speed and wind direction at 5 m height at the Gaudergrat ridge (a) in the lee slope close to the ridge (b) for the nine hour period. Shown are 1 h average values.

Figure 3 summarizes the measured time development of mean wind speed and direction at the ridge (Figure 3a) and in the lee slope (Figure 3b) for a part of our drift period studied. We select the precipitation period of January 28 to demonstrate the effect of preferential deposition. We divide the 9-hour period in three parts of 3 hours each and only use one wind-field per sub-period. We further select arbitrarily a model grid point on top of the ridge and the next grid point in the lee slope.

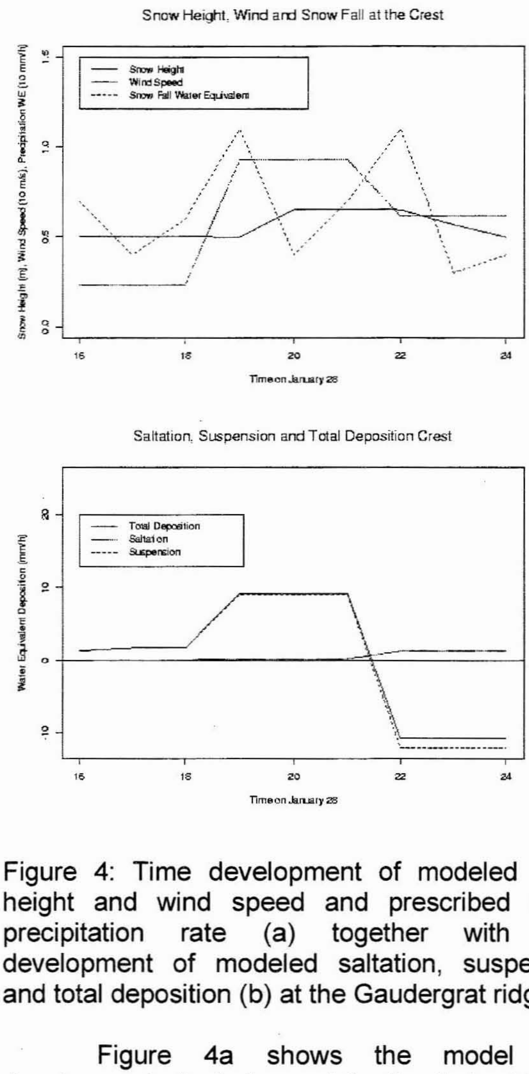

Figure 4: Time development of modeled snow height and wind speed and prescribed mean precipitation rate (a) together with time development of modeled saltation, suspension and total deposition (b) at the Gaudergrat ridge.

Figure 4a shows the model time development of wind speed for the first grid level (approximately 1 m over ground) at the ridge top. The curve is a simplified reconstruction of the measured wind speed (Figure 3a). Also shown in Figure 4a are the upper-level mean precipitation rate, which is prescribed as the upper (and lateral) boundary condition for the suspension model. The snow cover is initialized with 0.5 m of old snow. The time development of the snow height shows that during the first sub-period, no snow is deposited at the crest. During the following period, some snow is deposited and the snow height increases to 0.65 m. This snow is then eroded again during the third sub-period. In Figure 4b the deposition and erosion rates are given. Note that the snow model only reacts to changes in snow depth larger than 10 cm. Therefore the small total deposition rate (Figure 4b) during the first sub-period (which is entirely due to suspension) is not represented in a (very small) snow height increase in Figure 4a. The deposition rate increases during the second sub-period and even a very small contribution of saltation is observed. During the third period, saltation is present and snow is eroded. Note that the (total) erosion and deposition rates are comparable to the precipitation rate (Figure 4a).

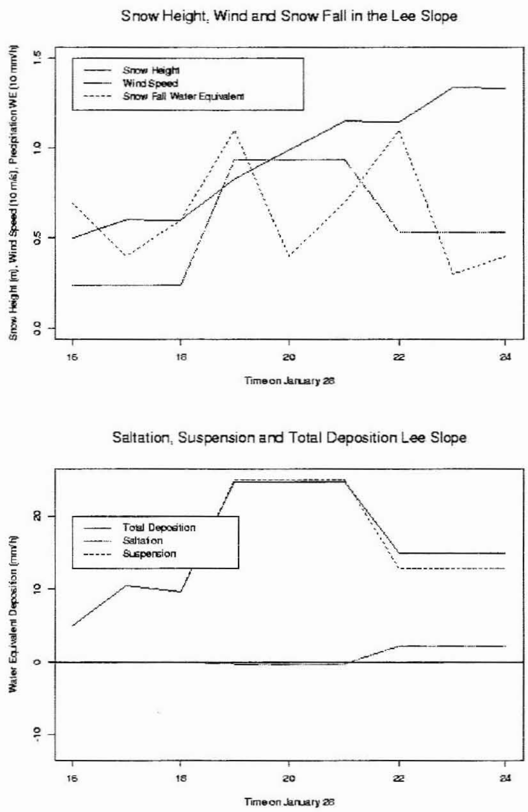

Figure 5: Time development of modeled snow height and wind speed and prescribed mean precipitation rate (a) together with time development of modeled saltation, suspension and total deposition (b) in the lee slope 25 m from the ridge.

The situation at the grid point in the lee slope is presented in Figure 5. During the whole period, the snow depth increases by almost 1 m (Figure 5a). Of particular interest is the first sub-period, where wind speeds are low and no saltation is occurring. Already during these first three hours, the deposition rates in the lee slope are 5 to 10 times higher (Figure 5b) than at the crest (Figure 4b). Preferential deposition significantly influences the build-up of the snow cover. During the second sub-period, where a negligible contribution of saltation is calculated, approximately 2.5 times more snow is deposited in the lee slope (Figure 5b) than at the crest (Figure 4b). During the third sub-period, a non-negligible influence of saltation is calculated. Deposition of snow continues in the lee slope, while at the crest the previously deposited snow is eroded again.

4. CONCLUSIONS

The complete model system consisting of an atmospheric flow model (ARPS) and model modules for suspension, saltation and snow cover development simulates with very encouraging. accuracy mass deposition of snow for a snow drift case in steep Alpine terrain. Since all model parts are based on physical process descriptions, we further investigated the role of different processes to the overall mass transport. For our situation at the steep Gaudergrat ridge, saltation appears to be less important than commonly assumed. Snow redistribution appears to be mainly due to suspension. It is particularly emphasized that during snow fall events snow is already unevenly distributed, even when the wind velocities are too small for erosion of already deposited snow and thus the saltation layer is missing. For a selected time span of three hours within a real drift period during snow precipitation, between 2.5 and 10 times more snow is deposited in lee slopes than at wind-exposed sites. We call this process preferential deposition. Our findings of the relative importance of the mass transport processes are purely based on the model results. In the future, more experimental work is required to verify these predictions.

The snow cover model SNOWPACK is coupled to the drift modules and provides the threshold condition for saltation (Lehning et al., 2000a). It also receives the fresh snow from the drift module or provides snow to be eroded. Its full capacity will be effective when longer periods can be simulated and detailed snow cover development and lee and luff slopes can be modelled. This will not only be useful for the purpose of avalanche warning but also to study questions associated with the snow – vegetation interaction or water storage and meltwater production. The increased computer power necessary for such long term simulations will be made available using the emerging GRID technology.

The model system is under development and needs improvements. While the saltation model has been validated for flat terrain (Doorschot and Lehning, 2002), the validation of the individual model parts saltation as well as suspension for slopes is missing. Also the wind model is not yet simulating flow separation to its full observed extent (Raderschall et al., 2002). Our effort is devoted to a more complete understanding and verification of the individual process formulations. This includes the transition from saltation to suspension. More field experiments as well as laboratory experiments in a new cold wind tunnel in Davos are currently under way.

Acknowledgements

We thank Walter Ammann for his continuous support. The work is funded by the Swiss National Science Foundation, the Swiss Federal Institute for Snow and Avalanche Research as part of the Swiss Federal Institute for Forest, Snow and Landscape Research and the Council of the Swiss Federal Institutes of Technology. Part of the simulations were made using the Advanced Regional Prediction (ARPS) developed by the Center for Analysis and Prediction of Storms (CAPS), University of Oklahoma. CAPS is supported by the National Science Foundation and the Federal Aviation Administration through combined grant ATM92-20009.

5. REFERENCES

Andreas, E.L., 1995: Air-ice drag coefficients in the western Weddell Sea 2. A model based on form drag and drifting snow, *J. Geophys. Res.*, **100**, 4833-4843.

Bartelt, P.B. and M. Lehning, 2002. A physical SNOWPACK model for Avalanche Warning Services. Part I: Numerical Model, *Cold Reg. Sci. Technol.*, in press.

Bintanja, R. and M.R. Van den Broeke, 1995. Momentum and scalar transfer coefficients over aerodynamically smooth Antarctic surfaces, *Boundary-Layer Meteorol.*, **74,** 89 – 111.

Bintanja, R., 2000. Snowdrift suspension and atmospheric turbulence. Part I: Theoretical background and model description, *Boundary-Layer Meteorol.*, **95,** 343 - 368.

Déry, S.J., P.A. Taylor and J. Xiao, 1998. The thermodynamic effects of sublimating, blowing snow in the Atmospheric Boundary Layer, *Boundary-Layer Meteorol.*, **89**, 251-283.

Déry, S.J. and M.K. Yau, 2001. Simulation of blowing snow in the Canadian Arctic using double moment model, *Boundary-Layer Meteorol.*, **99**, 297 - 316.

Doorschot, J., Lehning, M., 2002. Equilibrium saltation: mass fluxes, aerodynamic entrainment and dependence on grain properties, Bound. Layer Meteorol., 104(1), 111-130.

Föhn, P.M.B., 1980: Snow transport over mountain crests, *J. Glaciol.*, **26**, 469-480.

Föhn, P.M.B. and R. Meister, 1983. Distribution of snow drifts on ridge slopes: Measurements and theoretical approximations, *Ann. Glaciol.*, **4**, 52-57.

Gallée, H., Guyomarc'h, G, Brun, E., 2001. Impact of snow drift on the Antarctic ice sheet surface mass balance: possible sensitivity to snow-surface properties, *Boundary-Layer Meteorol.*, **99**, 1 - 19.

Gauer, P., 2001: Numerical modelling of blowing and drifting snow in Alpine terrain, *J. Glaciol.*, **47**(156), 97 - 110.

Green, E.M., Liston, G.E. and Pielke Sr., R.A., 1999: Simulation of above treeline snowdrift formation using a numerical snow-transport model, *Cold Reg. Sci. Technol.,* **30**, 135-144.

King, J.C., Anderson, P.S., Smith, M.C., Mobbs. S.D., 1996. The surface energy and mass balance at Halley, Antarctica during Winter, **101**(D14), 19'119 – 19'128.

Lehning, M., Doorschot, J., Bartelt, P., 2000a: A Snow Drift Index Based on SNOWPACK Model Calculations, *Ann. Glac.,* **31**, 382-386.

Lehning, M., Doorschot, J., Raderschall, N., Bartelt, P., 2000b. Combining snow drift and SNOWPACK models to estimate snow loading in avalanche slopes, in Snow Engineering, Hjorth-Hansen, Holand, Loset & Norem (eds), *Balkema*, 113-122.

Lehning, M, Bartelt, P.B., Brown, R.L., Fierz, C., Satyawali, P., 2002a. A physical SNOWPACK model for the Swiss Avalanche Warning Services. Part II: Snow Microstructure, *Cold Reg. Sci. Technol.*, in press.

Lehning, M, Bartelt, P.B., Brown, R.L., Fierz, C., 2002b. A physical SNOWPACK model for the Swiss Avalanche Warning Services. Part III: Meteorological Boundary Conditions, Thin Layer Formation and Evaluation, *Cold Reg. Sci. Technol.*, in press.

Lehning, M., P. Bartelt, B. Brown, T. Russi, U Stöckli and M. Zimmerli. 1999. SNOWPACK model calculations for avalanche warning based upon a new network of weather and snow stations. *Cold Reg. Sci. Technol.*, **30**, 145-157.

Liston, G.E., Sturm, M., 1998: A snow-transport model for complex terrain, *J. Glaciol.*, **44**, 498-516.

Mann, G.W., Anderson, P.S., Mobbs. S.D., 2000. Profile measurements of blowing snow at Halley, Antarctica, *J. Geophys. Res.*, **105**(D19), 24'491 – 24'508.

Meister, R., 1987: Wind systems and snow transport in alpine topography; in avalanche formation, movement and effects, *IAHS Publ.*, **162**, 265-279.

Naaim, M., Naaim-Bouvet, F. and Martinez, H., 1998: Numerical simulation of drifting snow: erosion and deposition models, *Ann. Glaciol.*, **26**, 191-196.

Pomeroy, J.W. and Gray, D.M., 1990: Saltation of snow, *Water Resources Research*, **26**, 1583-1594.

Raderschall, N., Lehning, M., Doorschot, J., 2002: Boundary layer wind field over steep, snow covered high alpine topography, Proc. 10th Conference Mountain Meteorology, 303-306.

Schmidt, R.A., 1980: Threshold wind-speeds and elastic impact in snow transport, *J. Glaciol.*, **26**, 453-467.

Sundsbø, P.-A., 1998: Numerical simulation of wind deflection fins to control snow accumulation in building steps, *J. Wind Eng. Ind. Aerodyn.,* **74-76**, 543-552.

Uematsu, T., 1993: Numerical study on snow transport and drift formation, *Ann. Glaciol.*, **18**, 135-141.

Wamser, C., Lykossov, V.N., 1995: On the friction velocity during blowing snow, *Beitr. Phys. Atmosph.*, **68**, 85-94.

Xiao, J., Bintanja, R., Déry, S.J., Mann, G.W., Taylor, P.A., 2000. An intercomparison among four models of blowing snow, *Boundary-Layer Meteorol.*, **97**, 109 – 135.

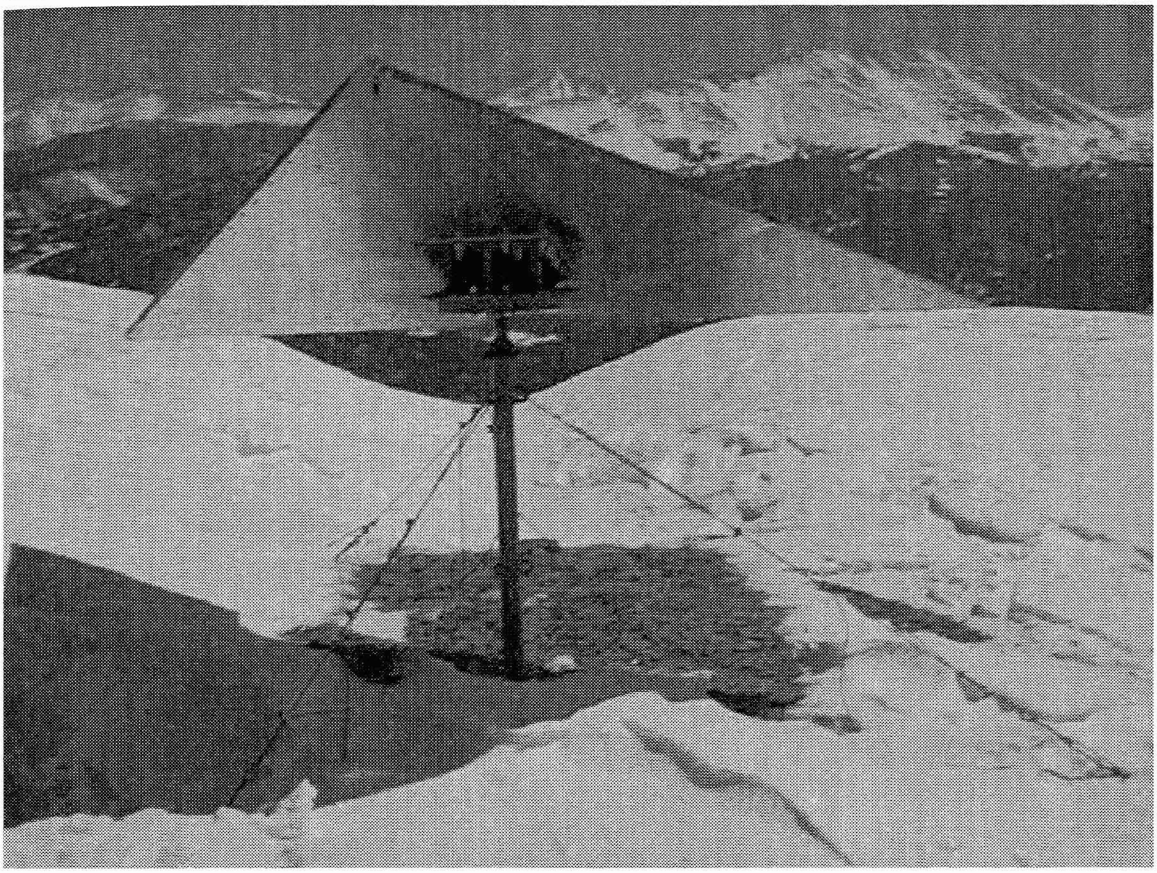

A CONTINUING STUDY OF VORTEX GENERATORS

A continuing study of the effect of vortex generators on cornice development. This is a photographic study over the past four years of how vortex generators have assisted in minimizing cornice development. Beginning with one generator in the winter of 1998 we have expanded to five generators along a corniced ridge approximately 450 meters long.

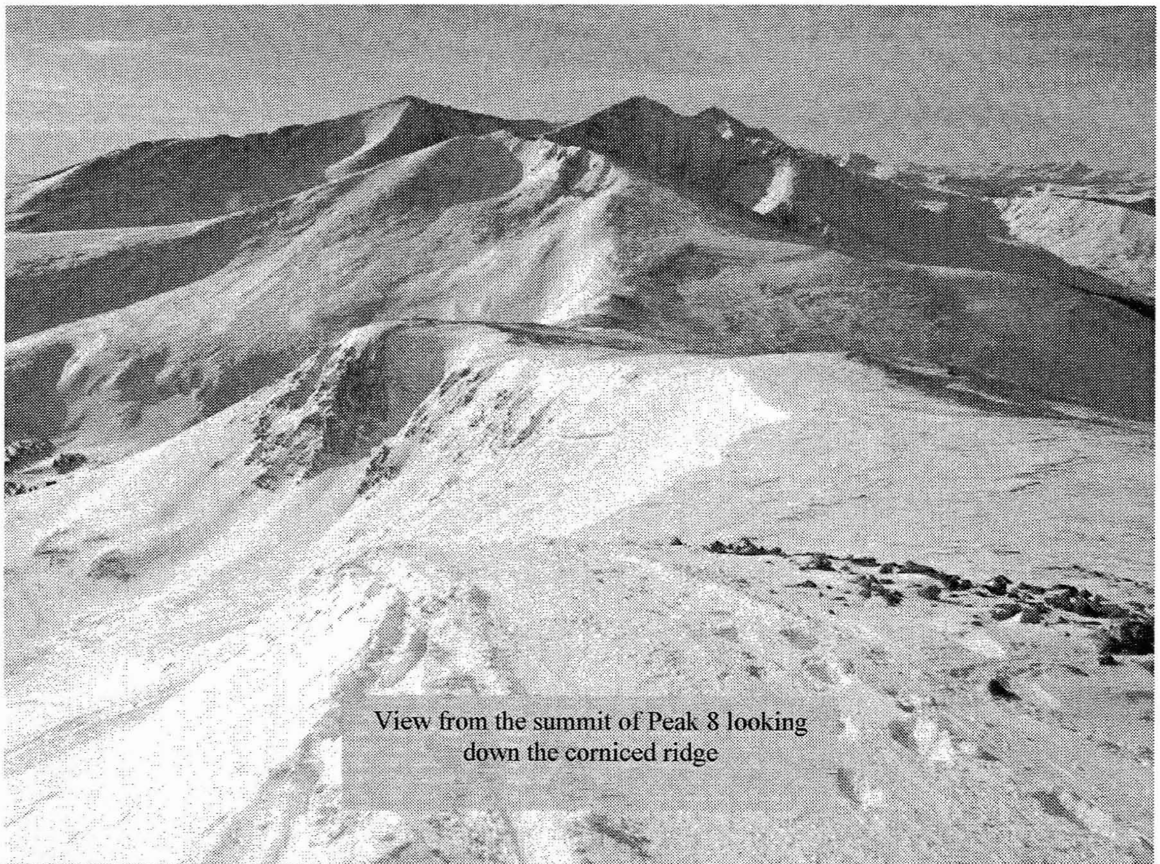

View from the summit of Peak 8 looking down the corniced ridge

Erosion in cornice created by vortex generator

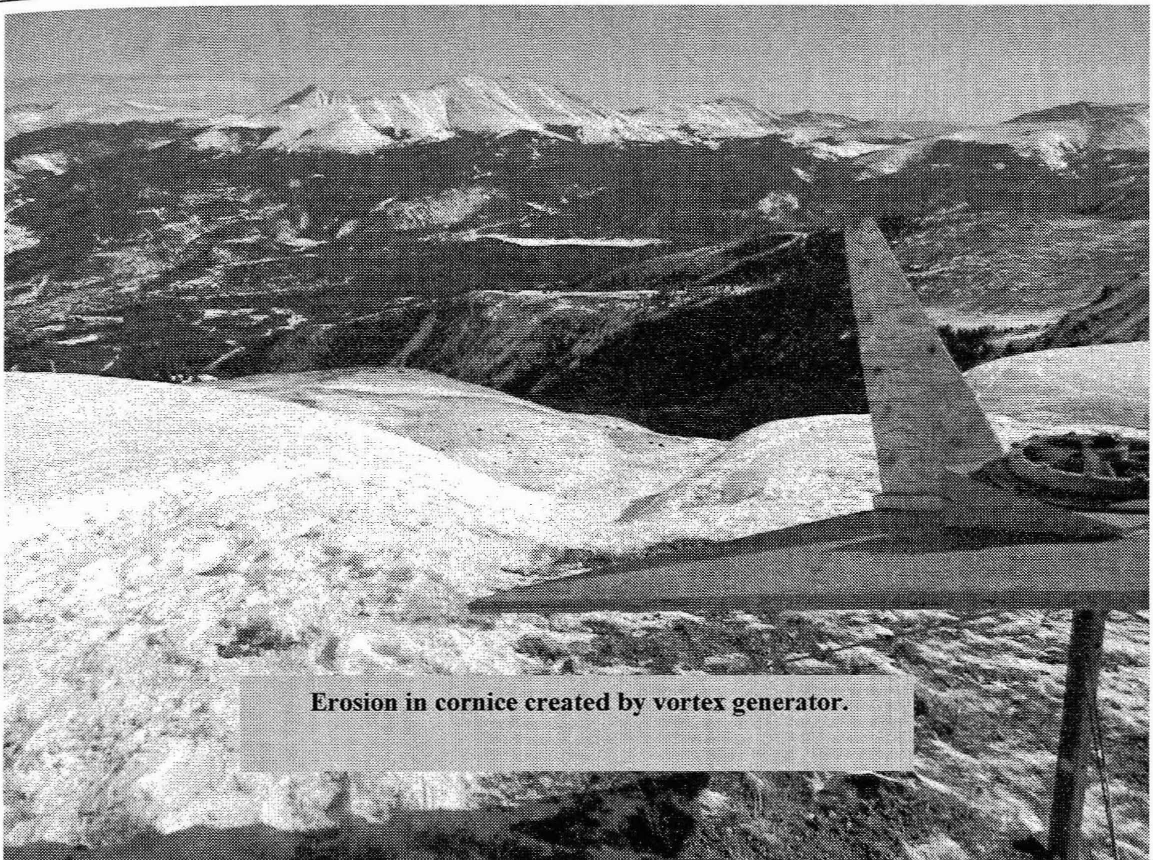

Erosion in cornice created by vortex generator.

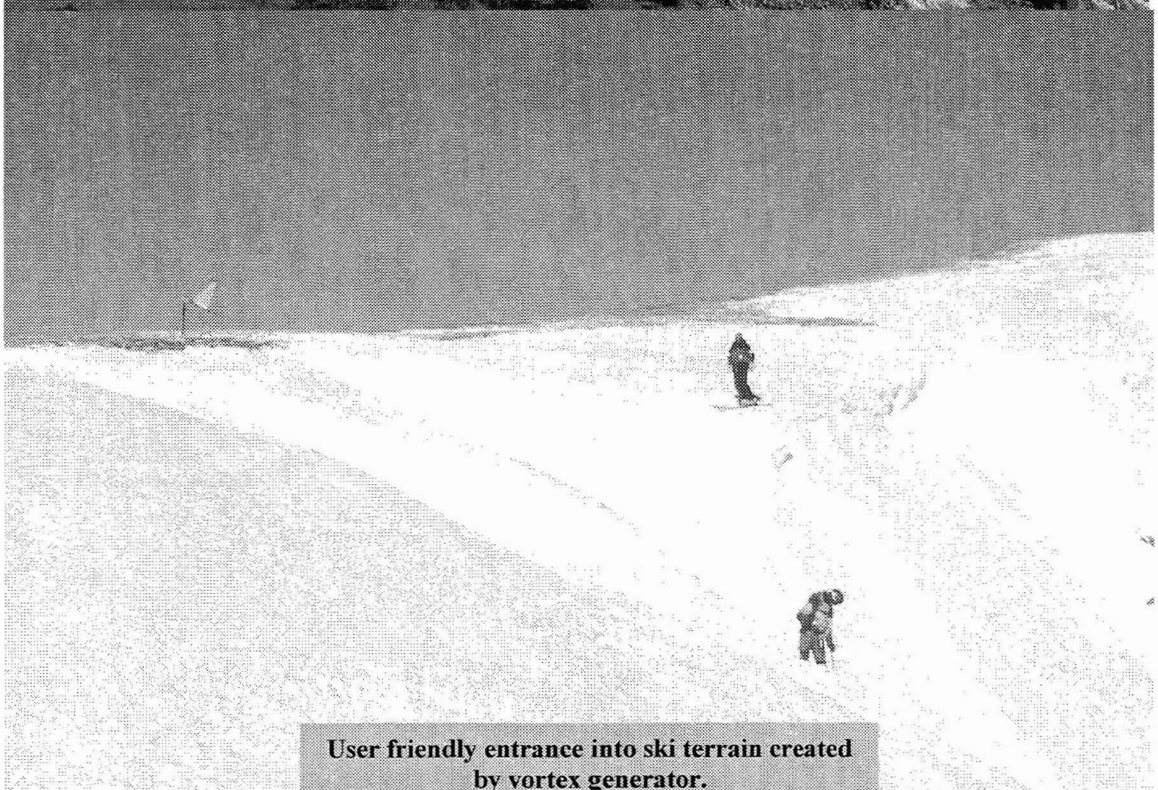

User friendly entrance into ski terrain created by vortex generator.